Evidence for cathodic protection of crystallographic facets from GaAs etching profiles

Evidence for Cathodic Protection of Crystallographic Facets from GaAs Etching Profiles

P. H. L. Notten and J. J. Kelly

Philips Research Laboratories, 5600 JA Eindhoven, The Netherlands

ABSTRACT

Etching experiments were carried out on partially masked GaAs single crystals in alkaline $K_3Fe(CN)_6$ solutions in which the dissolution rate of all crystal planes is diffusion-controlled. Etching could be rate determined in two ways. In the first case, mass transport of OH^- ions to the GaAs surface determined the rate of the anodic partial reaction and also the etch rate. This resulted in rounded profiles at the semiconductor/resist edge as expected for diffusion limited etching. In the second case, mass transport limited reduction of the oxidizing agent determined the dissolution rate. Etching at the resist edge was now, surprisingly, anisotropic and faceted profiles were observed. On the basis of electrochemical measurements with these etchants it is concluded that a local galvanic element can be formed between crystallographic facets. As a result, certain facets may be cathodically protected and consequently etch more slowly than the corresponding free crystal plane.

In previous work (1), we developed a mathematical model to describe diffusion-controlled etching at resist edges. When the rate constants for dissolution of a monocrystalline solid are very high for all crystallographic planes, then mass transport in the solution is generally rate determining, and etching is expected to be isotropic. At resist edges, therefore, rounded profiles are predicted, and the etch depth near the edge is enhanced because of a more efficient supply of etchant. This model was verified for GaAs using various chemical etchants (1). With electroless systems, however, we found anomalous results. In many cases in which the etch rate of the various crystal planes of GaAs was clearly diffusion controlled, etching at resist edges was, nevertheless, anisotropic (1).

In the present work, we described this etching anomaly. Results of current-potential and impedance measurements are used to assist in understanding the unusual etching results. The conclusions have, however, a wider relevance since they show the importance of electrochemical interaction between different crystallographic facets in a single crystal electrode.

Experimental

In this work we used n-type and p-type GaAs wafers with the (100), (111) Ga, and (111) As orientations. All samples were obtained from MCP Electronics, Limited, England and had a carrier concentration in the range 5×10^{17}-2×10^{18} cm^{-3}. The slices were mechano-chemically polished before use.

For the etching experiments either photoresist (HNR-999 and HPR-204 from Shipley) or SiO_2 were used to mask the GaAs surface. The samples were mounted on a glass plate and hung vertically in the etching solution. The etchants used are described in detail elsewhere (1). After etching, the slices were cleaved perpendicular to the resist edge, and the etched profiles were examined in a scanning electron microscope (SEM). The resist layer was not removed in these experiments, and consequently the overhanging edge can be seen in the SEM photos.

The experimental details for the electrochemical measurements were the same as those reported in previous work (2). Potentials are given with respect to the saturated calomel electrode (SCE). All measurements were performed at room temperature.

The Etching Anomaly

Figure 1a shows a profile at the resist edge obtained with a GaAs sample in a diffusion-controlled etchant ($HCl/H_2O_2/H_2O$). This is a typical chemical etching system: a synchronous exchange of bonds occurs between a Ga-As surface pair and the etching species, H_2O_2 in this case (1). Free charge carriers are not involved in this reaction, and the etch rate is not influenced by an applied potential. The excellent agreement between the measured result and that predicted by the two-dimensional diffusion model is shown in Fig. 1b.

For electroless systems, etching occurs at a mixed potential which is determined by two potential dependent electrochemical reactions: oxidative dissolution of the solid and reduction of an oxidizing agent in solution. The holes required for GaAs dissolution are supplied by the oxidizing agent. The etch rate can be diffusion controlled in two different ways (1). The most common case is that in which the reduction reaction is diffusion limited and controls the etching kinetics. The result of an etching experiment with such a solution is given in Fig. 2a. Despite the fact that the macroscopic etch rate of all crystal faces was shown to be diffusion controlled, a rounded profile was not observed at the resist edge. Instead, a clearly defined crystallographic facet was ex-

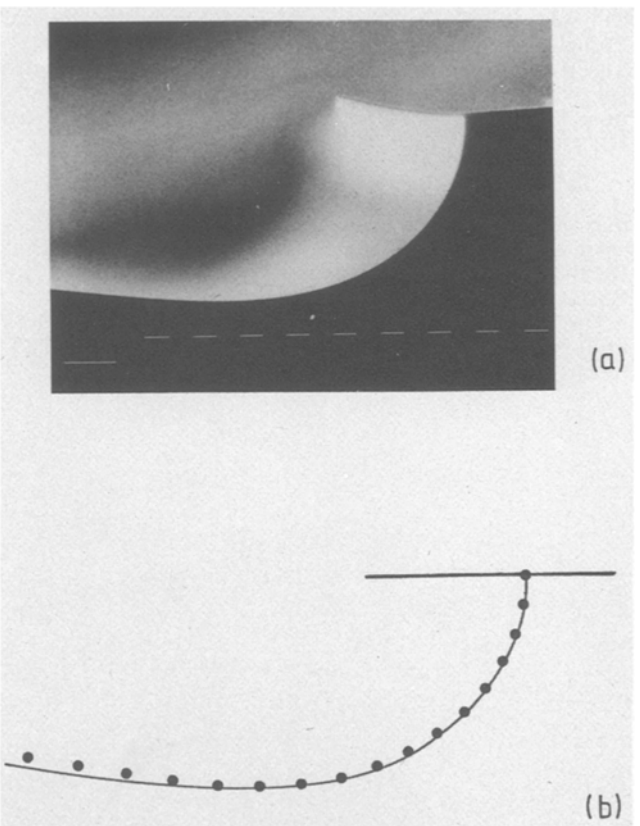

Fig. 1. a. SEM photo of a profile etched in (100) GaAs using a $HCl/H_2O_2/H_2O$ solution. The volume ratio of HCl (37%) to H_2O_2 (30%) was 40/1. The etching time was 5 min. b. Shows the agreement between the profile measured in 1a (continuous line) and that calculated from theory (filled circles). One white bar corresponds to 1 μm.

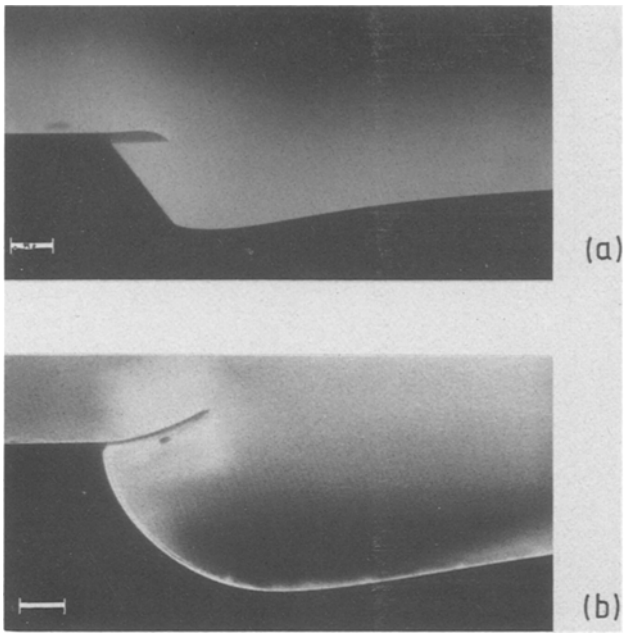

Fig. 2. Profiles obtained in n-type (100) GaAs using $K_3Fe(CN)_6$ solutions at pH 13: (a) 0.05*M* $K_3Fe(CN)_6$, etching time 10 min; (b) 0.5*M* $K_3Fe(CN)_6$, etching time 10 min. The white bar corresponds to 2 μm.

posed during dissolution; in this case it was the (111) Ga face. Similar results were found with analogous etchants, *e.g.*, Ce^{4+} solutions at low *p*H.

We have shown that, under certain conditions, etching may also be mass transport controlled via the anodic reaction (1). At high *p*H, the maximum rate of anodic dissolution of GaAs depends on diffusion of OH^- ions to the electrode. Electroless etchants based on this limitation show a profile typical of diffusion-controlled dissolution (Fig. 2b). This form agrees with that predicted by theory, as comparison with Fig. 1 clearly shows.

The results given in Fig. 2, which are typical of both n- and p-type materials, are striking in two respects: etching, when diffusion controlled via the reduction reaction, invariably gives a faceted (anisotropic) profile while a slight variation in etchant composition is sufficient to make the system isotropic.

In subsequent sections, we shall consider the electrochemistry of these etching systems at GaAs electrodes and the influence of crystallographic orientation on the reactions.

Results and Discussion

Influence of etchant composition on electrochemical results.—The essential difference between the two solutions used for the etching experiments of Fig. 2 can be illustrated most simply by considering current-potential curves at p-type GaAs. In Fig. 3 results are shown for a (100) electrode in 0.05*M* $Fe(CN)_6^{3-}$ solution at *p*H 13. The total current-potential curve (a) shows three distinct plateaus. Using a ring-disk electrode, it is possible to determine the partial cathodic current due to $Fe(CN)_6^{3-}$ reduction (curve b)

$$Fe(CN)_6^{3-} \rightarrow Fe(CN)_6^{4-} + h^+ \qquad [1]$$

At negative potentials the reduction reaction is diffusion controlled and the cathodic current is consequently potential independent. Reduction stops at a potential close to the redox potential of the $Fe(CN)_6^{3-}/Fe(CN)_6^{4-}$ couple (3).

On substracting the cathodic current from the total current, we obtain the partial anodic curve (c) due to GaAs oxidation (4)

$$GaAs + 10\ OH^- + 6h^+ \rightarrow GaO_2^- + AsO_3^{3-} + 5H_2O \qquad [2]$$

This reaction becomes important at potentials near the

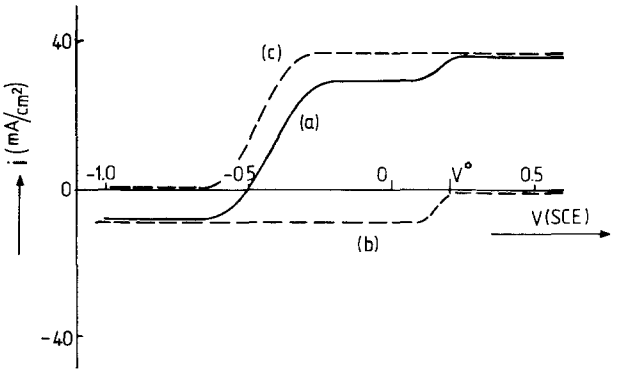

Fig. 3. Current-potential curves for a p-type (100) GaAs electrode in 0.05*M* $K_3Fe(CN)_6$ solution at *p*H 13: (a) total curve; (b) and (c) are the cathodic and anodic partial curves. Electrode rotation rate: 200 rpm.

flatband value (V_{FB}). At more positive potentials, the anodic partial current also becomes constant. We have shown that, in this case, dissolution depends on transport of OH^- ions to the electrode surface (1, 3). The intermediate plateau observed in the total curve is due simply to the difference between the potential-independent anodic and cathodic curves.

The limiting anodic partial current is considerably larger than the corresponding cathodic current. It follows, therefore, that the etching kinetics at the rest potential are determined by the reduction of the oxidizing agent.

A similar current-potential curve (Fig. 4) is observed with the electrolyte used for isotropic etching in Fig. 2b. However, since in this case the $Fe(CN)_6^{3-}$ concentration is a factor of 10 higher, the limiting cathodic current is now larger than the corresponding anodic current. The etch rate is therefore determined by the anodic reaction, *i.e.*, OH^- diffusion, and the rest potential of the system is considerably more positive than that found for the previous case in Fig. 3.

Influence of crystallographic orientation on electrochemical results.—It is well established that different crystallographic orientations of III-V materials can differ considerably in electrochemical properties. In Table I we give the values of the flatband potential for our n-type and p-type GaAs electrodes. These results, measured in 0.1*N* NaOH solution, are self-consistent; the difference between V_{FB} values of n- and p-type samples of the same crystallographic orientation is close to the bandgap of GaAs as expected (5). While the (100) and (111) As electrodes have quite similar flatband potentials, the value for the (111) Ga face is considerably more positive. Rajeshwar and Mraz have also shown for n-type GaAs

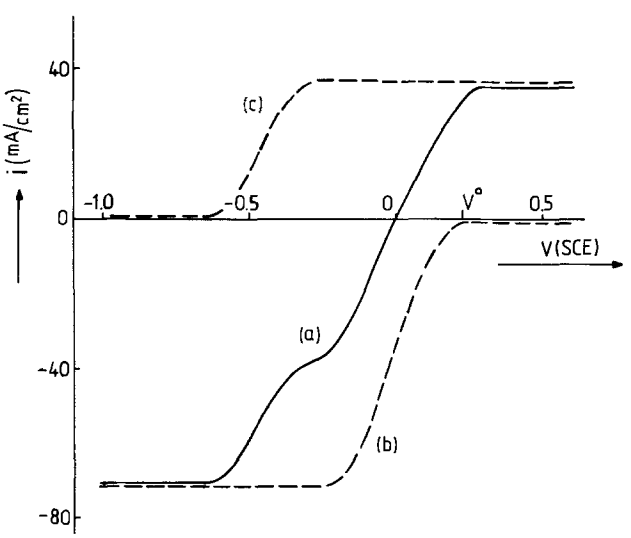

Fig. 4. Current-potential curves for a p-type (100) GaAs electrode in 0.5*M* $K_3Fe(CN)_6$ at *p*H 13. The notation is the same as for Fig. 3.

Table I. The influence of crystallographic orientation on the flatband potential of GaAs electrodes in 0.1N NaOH solution. V_{FB} is given in volts vs. SCE

	n-type	p-type
(100)	−1.80	−0.50
(111) As	−1.75	−0.45
(111) Ga	−1.55	−0.25

that both the flatband potential and its pH dependence depend markedly on the orientation (6). The V_{FB} value of the (111) Ga face was generally more positive than that of the (111) As and (100) faces. Such effects can be understood in terms of differences in the Helmholtz layer (6).

The difference in V_{FB} values shown in Table I are also reflected in the anodic current-potential curves. In Fig. 5 results are shown for (111) Ga and (111) As surfaces of p-type material. Anodic dissolution of the Ga face starts at a potential more than 100 mV positive with respect to that of the As face. Differences in current-potential curves of n-type electrodes were also observed for different orientations.

Galvanic element formation and cathodic protection.— When a single crystal is etched at a resist edge, various crystal faces can be exposed to the solution. It is clear from the results described above that such faces differ in electrochemical activity. The importance of crystallographic orientation for etching kinetics has long been recognized. The A face of III-V crystals generally etches more slowly than the other faces, when dissolution is not diffusion controlled (7). Gatos reports that the rest potential of A surfaces in oxidizing etchants is more positive than that of the other surfaces (7). In electrochemical terms all these results mean that the A face is, as a rule, more "noble." Such a difference in nobility suggest the possibility of local element formation (8, 9) between crystallographic facets. It has been shown above that the rest potential of the electrode depends markedly on the electrolyte composition. Differences in rest potential can have an important influence on the etching results in the case of local element formation in metals (9).

The effects are illustrated schematically in Fig. 6 and 7 for p-type material. For Fig. 6 it is assumed that reduction of the oxidizing agent is diffusion limited. Here we consider two arbitrary crystal planes, denoted by A and B. The difference in nobility is indicated by the difference in potential for anodic current onset. For simplicity, we ignore any diffusion limitation on the anodic side, and we assume that the areas of each plane exposed to the etchant are the same. It is clear that at the separate rest potentials V_A and V_B, the etch rates of the two planes are the same, being controlled by diffusion of the oxidizing agent. When the two surfaces are brought into

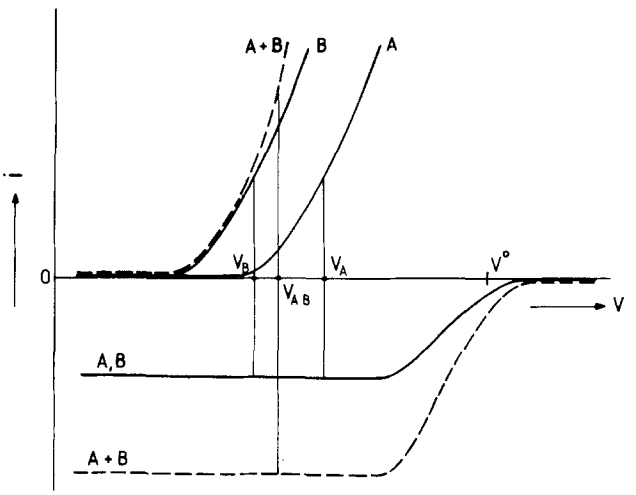

Fig. 6. Schematic representation of galvanic element formation between two crystal planes, A and B. The solid lines give the partial current-potential curves for the individual planes. The dashed lines refer to the total anodic and cathodic curves for the two planes in electrical contact. The mixed potentials of the individual planes in the solution are indicated by V_A and V_B. V_{AB} is the value for the combined system. In this example, reduction of the oxidizing agent is diffusion controlled.

electrical contact, it is necessary to consider the total anodic and total cathodic current-potential curves (dashed lines, Fig. 6). The new rest potential V_{AB} lies between the values for the individual surfaces. It is assumed that the electrical resistance within the solid is negligible. Since V_{AB} is negative with respect to V_A and positive with respect to V_B, the etch rate of the more noble surface is diminished while that of the less noble surface is enhanced. In fact, holes supplied to the A face are used to etch preferentially the B face.

Although the case shown in Fig. 6 is, of course, oversimplified, it nevertheless illustrates how certain facets can be cathodically protected by the neighboring surface. This model can therefore explain why a faceted profile is obtained even though the individual free planes are etched at a diffusion-controlled rate.

In Fig. 7 the alternate case is considered in which a limiting anodic reaction determines the etching kinetics. In this case, since the cathodic diffusion current is sufficiently large, it need not be included in the figure. The difference in nobility between the A and B planes is again clear from the anodic current onset. On the basis of this figure one can conclude that, because the anodic current is potential independent, the etch rates of the A and B planes are not affected when the two surfaces are

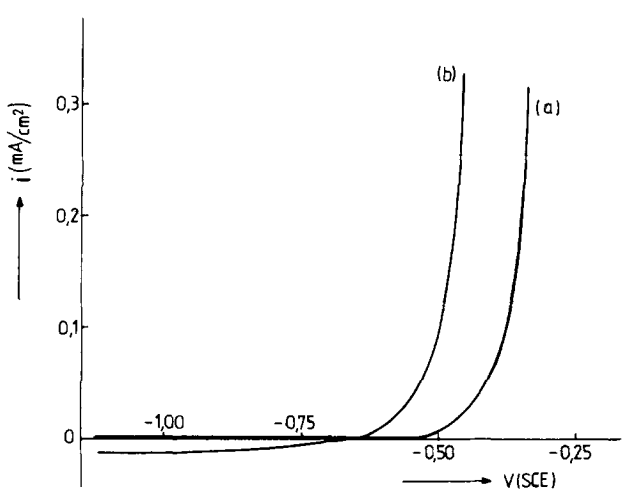

Fig. 5. Current-potential curves for a p-type (111) GaAs electrode in 0.1N NaOH solution. Curve (a) refers to the (111) Ga face, (b) to the (111) As face.

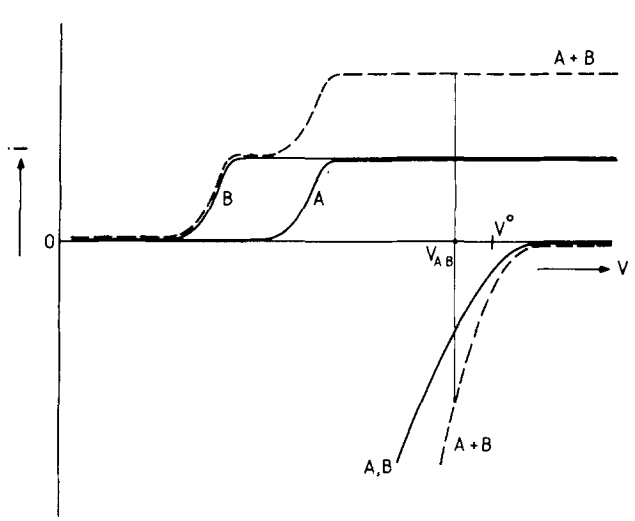

Fig. 7. Galvanic element formation between two crystal planes, A and B, for the case in which oxidation of the solid is diffusion controlled. The notation is the same as for Fig. 6.

connected electrically. It is clear that in this case the more noble surface is not cathodically protected. In fact all surfaces are dissolved at the same rate, which is determined by OH^- diffusion. Etching at resist edges is expected to be isotropic. This is, indeed, what we observe (see Fig. 2b).

If this analysis is correct, then the form of the GaAs profiles etched in alkaline $Fe(CN)_6^{3-}$ solutions should be determined by the ratio of the anodic and cathodic limiting currents, *i.e.*, by the ratio of the OH^- and $Fe(CN)_6^{3-}$ concentrations. The change in profile in Fig. 2 was brought about at a fixed *p*H by increasing the concentration of the oxidizing agent.

The importance of the solution *p*H is shown in Fig. 8. Measured current-potential curves are given for a constant $Fe(CN)_6^{3-}$ concentration. These curves fall into two groups. At relatively low *p*H, the limiting anodic current is smaller than the cathodic current. Etching is determined by OH^- diffusion and a relatively positive rest potential ($\geq$ 0.0V SCE) is found. At higher *p*H, the situation is reversed and reduction of the oxidizing agent is the determining reaction. The rest potential is approximately 300 mV more negative than in the previous case. The two kinetic groups of Fig. 8 correspond to the two cases of etching morphology. The rounded profile shown in Fig. 9a was obtained with a 0.5*M* $K_3Fe(CN)_6$ solution of *p*H 13 (see also Fig. 2b). The profile can be made anisotropic simply by raising the etchant *p*H from 13 to 14 (Fig. 9b).

The description of p-type GaAs given so far is similar to that which can be used for the corrosion of metals (11). For an n-type material the situation is less straightforward. In this case the oxidizing agent injects minority carriers (holes) into the valence band of the solid. These holes are used to dissolve the semiconductor. During the oxidation of GaAs, surface-state intermediates are formed, and these can, to a small extent, inject electrons into the conduction band (10). At the open-circuit potential, these electrons and holes must recombine. Because of differences between the rates of hole injection and hole consumption, charging of the semiconductor/electrolyte interface is observed (3). The rest potential of n-type GaAs in an etching system is therefore determined by a complex combination of all these factors (10). Electrochemical measurements with n-type electrodes in the electrolytes described above show, however, features similar to those found for p-type GaAs (3). When the $Fe(CN)_6^{3-}$ concentration is high in comparison to the OH^- concentration, etching is anodically controlled, and the etch rate is determined by OH^- diffusion to the GaAs surface. On the other hand, when the $Fe(CN)_6^{3-}$ concentration is relatively low, the cathodic reaction involving diffusion of the oxidizing agent controls the etching kinetics. Again a considerable difference in the rest potential is observed for the two cases. The crystallographic orientation has an important effect. So although it is not easy to predict the rest potential and the potential distribution, it nevertheless seems reasonable to expect that local elements can also be formed in a multifaceted n-type system and that certain facets can be cathodically protected. This has, indeed, been found experimentally.

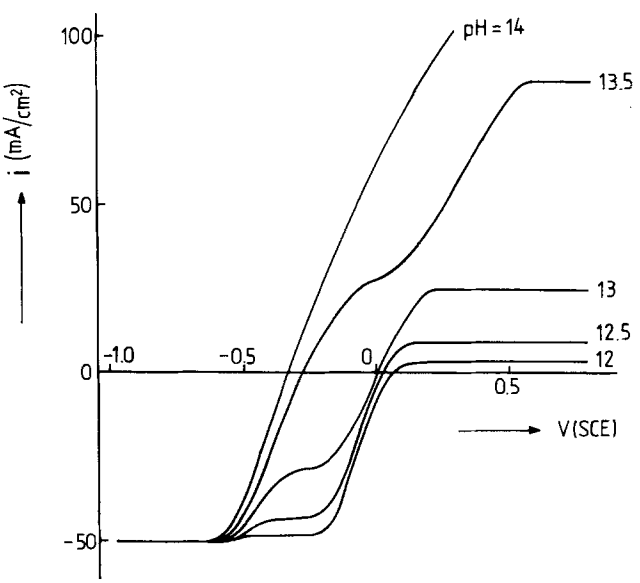

Fig. 8. Current-potential curves for a p-type (100) GaAs electrode in 0.5*M* $K_3Fe(CN)_6$ solution as a function of *p*H (indicated on the curves). The electrode rotation rate was 100 rpm.

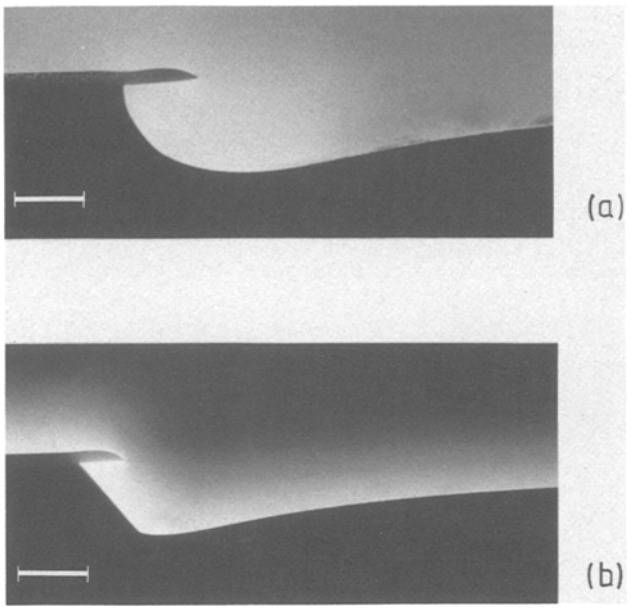

Fig. 9. Profiles obtained in n-type (100) GaAs using a 0.5*M* $K_3Fe(CN)_6$ solution: (a) at *p*H 13, etching time 10 min; (b) at *p*H 14, etching time 2 min. The white bar corresponds to 5 μm.

Conclusions

The etching results described in this work lead us to conclude that local galvanic elements can be formed between crystallographic facets of monocrystalline materials. Such element formation can have important consequences for the application of these materials.

In the absence of galvanic interaction between facets, one would always expect rounded profiles at resist edges when the etch rate of all crystal planes of the solid is diffusion-controlled. This we clearly observe with chemical etchants. In this case, etching is based on a local bond exchange mechanism. On the other hand, for electroless etching in which free charge carriers are important, galvanic interaction can occur between facets. The specific etching mechanism is then decisive for the form of the etched profile. If the etching kinetics are determined by a diffusion-controlled reduction of the oxidizing agent and the facets differ in electrochemical "nobility," then cathodic protection of the nobler facets is observed. When rounded profiles are required, this galvanic effect can be avoided by choosing an etchant based on a diffusion-limited oxidation of the semiconductor.

Such galvanic elements can, in a similar way, influence the corrosion properties of semiconductor materials. Since crystallographic defects correspond to disturbed regions of the solid they are expected to be less noble than the surrounding material (11). We have, indeed, observed enhanced corrosion of such defects as a result of local element formation. This effect may be useful, if one is interested in revealing defects or removing defective regions. However, in the case of devices, localized etching due to galvanic effects at crystallographic imperfections is obviously undesirable. The present work presents ways in which such effects can be avoided.

Acknowledgments

The authors wish to thank Mrs. A. C. Reijnders for assisting with the measurements and J. E. A. M. van den Meerakker for helpful discussions.

Manuscript submitted April 29, 1986.

Philips Research Laboratories assisted in meeting the publication costs of this article.

REFERENCES

1. H. K. Kuiken, J. J. Kelly, and P. H. L. Notten, *This Journal*, **133**, 1217 (1986).
2. J. J. Kelly and P. H. L. Notten, *Electrochim. Acta*, **29**, 589 (1984).
3. P. H. L. Notten, *ibid.*, **00**, 000 (1986).
4. H. Gerischer, *Ber. Bunsenges. Phys. Chem.*, **69**, 578 (1965).
5. R. Memming, *This Journal*, **116**, 785 (1969).
6. K. Rajeshwar and T. Mraz, *J. Phys. Chem.*, **87**, 742 (1983).
7. H. C. Gatos, *Science*, **137**, 311 (1962).
8. K. J. Vetter, "Electrochemical Kinetics," Ch. 5, Academic Press, New York (1967).
9. J. J. Kelly and C. H. de Minjer, *This Journal*, **122**, 931 (1975).
10. H. Gerischer and I. Wallem-Mattes, *Z. Phys. Chem. N.F.*, **64**, 187 (1969).
11. K. W. Frese, M. J. Madou, and S. R. Morrison, *J. Phys. Chem.*, **84**, 3172 (1980).

Chemical Etching Characteristics of InGaAs/InP and InAlAs/InP Heterostructures

Alessandro Stano

CSELT—Centro Studi e Laboratori Telecomunicazioni, 10148 Torino, Italy

ABSTRACT

The chemical etching characteristics of (001) MBE and LPE InGaAs and InAlAs layers grown on InP have been studied for various etching systems: H_3PO_4: H_2O_2, H_2SO_4:H_2O_2:H_2O, and Br_2-CH_3COOH using photoresist as a mask. The etch profiles were examined on stripes oriented along the [110] and [1$\bar{1}$0] directions and on circular mesa structures. The etch rates and the etch-revealed planes are reported, together with a detailed discussion of the crystallography. Experimentally observed different etching characteristics between LPE and MBE InGaAs layers are reported and discussed. The use of these etching solutions for device fabrication is also briefly discussed.

The InGaAs and InAlAs ternary alloys, lattice matched to InP, are currently of great interest for a variety of high speed and optoelectronic devices. Furthermore, they are the two ternary limits of the InGaAlAs quaternary system, which is very promising for fiber and integrated optics applications.

Wet chemical etching and selective chemical etching are important methods in device fabrication. Several etching solutions have been used for InGaAs-based device fabrication: H_2SO_4:H_2O_2:H_2O (1-5) and Br_2-CH_3COOH (6), to define mesa structures for photodiodes, heterobipolar transistors, and for JFET's gate formation, and citric acid and H_3PO_4:H_2O_2:H_2O for JFET's and DH-MESFET fabrication (7-8). Conway *et al.* (9) have reported etch rates for a selective KOH:$K_3Fe(CN)_6$:H_2O etching solution for the InGaAs/InP system. However, to our knowledge, there has been no detailed report on InGaAs and InAlAs etching characteristics, such as device shaping, etch revealed planes, and etch rates, and only limited data on mesa tapering by several different etches have been reported (10).

In this paper, we report detailed experimental results on the chemical etching characteristics of MBE and LPE InGaAs/InP and MBE InAlAs/InP lattice-matched heterostructures in the solutions of three etching systems: (*i*) H_3PO_4, (*ii*) H_2SO_4, and (*iii*) Br_2-CH_3COOH. The etching profiles are examined by cleaving the (001) oriented InGaAs/InP and InAlAs/InP wafers in orthogonal planes along the [110] and [1$\bar{1}$0] directions and are discussed in detail from a crystallographic aspect, together with the etching profiles of circular mesa structures.

Experimental

Sample.—The samples employed were lattice-matched InGaAs and InAlAs heterostructures grown on (001) InP dislocation-free substrates.

The InGaAs samples were grown either by MBE (Si-doped, 10^{18} cm^{-3}), with the growth conditions previously described (11, 12), or by LPE (Sn-doped, 10^{18} cm^{-3}), while the InAlAs samples were grown by MBE (Si-doped, 10^{18} cm^{-3}) (13).

The samples were thinned to about 100 μm to permit cleavage for the observation of the etching profiles. Before mask deposition, the samples were degreased in organic solvents, deoxided in 40% HF, and then rinsed in deionized water.

Masking pattern.—Etching studies were performed on the (001) InGaAs and InAlAs surface after the realization of the masking pattern (see Fig. 1) by standard photolithographic techniques using Hunt HNR 999 negative photoresist baked at 120°C for 30 min.

This geometry allows the simultaneous observation of the etching profiles in the [110] and [1$\bar{1}$0] directions and on circular mesa shapes, where a continuous series of crystallographic planes are present.

Etching solutions.—For device applications, the etching solutions must exhibit oxidizing characteristics and must be free of metallic cations to avoid ionic contamination of the etched surface, which may produce undesired surface current leakage in device applications.

The chemical etching characteristics of InGaAs and InAlAs were studied in the solutions of three etching systems: (*i*) H_3PO_4:H_2O_2, (*ii*) H_2SO_4:H_2O_2:H_2O, and (*iii*) Br_2-CH_3COOH. All the etching experiments were performed at room temperature without stirring. Under these conditions, the first two systems are selective for both the InGaAs/InP and InAlAs/InP heterostructures.

The electronic grade reagents are in the following concentrations: H_3PO_4 (86%), H_2SO_4 (96%), H_2O_2 (33%), CH_3COOH glacial. The etching depths were measured by a

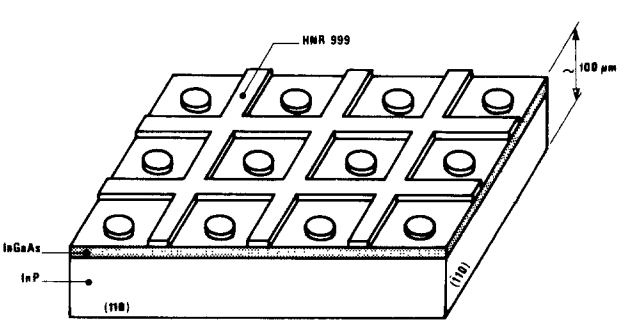

Fig. 1. Photoresist masking pattern on (001) InGaAs or InAlAs surface used for chemical etching experiments.